



Contents lists available at ScienceDirect

Virology

journal homepage: www.elsevier.com/locate/yviroAn antiviral RISC isolated from *Tobacco rattle virus*-infected plantsJessica J. Ciomperlik¹, Rustem T. Omarov², Herman B. Scholthof^{*}

Department of Plant Pathology and Microbiology, Texas A&M University, 2132 TAMU, College Station, TX 77843, USA

ARTICLE INFO

Article history:

Received 26 August 2010
 Returned to author for revision
 12 September 2010
 Accepted 13 December 2010
 Available online 26 January 2011

Keywords:

Silencing
 Virus
 RISC

ABSTRACT

The RNAi model predicts that during antiviral defense a RNA-induced silencing complex (RISC) is programmed with viral short-interfering RNAs (siRNAs) to target the cognate viral RNA for degradation. We show that infection of *Nicotiana benthamiana* with *Tobacco rattle virus* (TRV) activates an antiviral nuclease that specifically cleaves TRV RNA *in vitro*. In agreement with known RISC properties, the nuclease activity was inhibited by NaCl and EDTA and stimulated by divalent metal cations; a novel property was its preferential targeting of elongated RNA molecules. Intriguingly, the specificity of the TRV RISC could be reprogrammed by exogenous addition of RNA (containing siRNAs) from plants infected with an unrelated virus, resulting in a newly acquired ability of RISC to target this heterologous genome *in vitro*. Evidently the virus-specific nuclease complex from *N. benthamiana* represents a genuine RISC that functions as a readily employable and reprogrammable antiviral defense unit.

© 2011 Elsevier Inc. All rights reserved.

Introduction

RNA interference (RNAi) or silencing is a highly conserved molecular mechanism known to regulate gene expression and/or combat invasive nucleic acids across species including plants (Baulcombe, 2004), fungi (Romano and Macino, 1992), insects (Hammond et al., 2001) and mammals (Liu et al., 2004). As RNAi pathways were initially studied most intensely in *Drosophila melanogaster* and mammalian cells, accordingly the original RNAi models were based on those systems. Recently, these have been substantially augmented by (reverse) genetic studies using *Arabidopsis* (Li and Ding, 2006; Voinnet, 2005).

In the current RNAi model, the process is triggered by the presence of double-stranded RNA (dsRNA) structures; for instance, those that accumulate in the cell via viral infection or upon artificial introduction (Filipowicz, 2005). A Dicer protein cleaves these dsRNAs into smaller segments, giving rise to short duplex RNAs such as microRNAs (miRNAs) or short-interfering RNAs (siRNAs), with one strand of these used to program a multi-protein RNA-induced silencing complex (RISC). The programmed RISC then targets single-stranded (ss) RNAs complementary to the incorporated RNA for cleavage or translational repression, resulting in post-transcriptional silencing of specific genes.

RISC is postulated to be a high-molecular weight complex composed of at least one protein from the Argonaute (Ago) family, and possibly one Dicer family protein (MacRae et al., 2008; Song and

Joshua-Tor, 2006; Tomari et al., 2007). Ago proteins represent the catalytic effector unit(s) of RISC, and as such, are signature proteins of this pathway (Baumberger and Baulcombe, 2005; Hammond et al., 2001). Two protein domains, Piwi–Argonaute–Zwille (PAZ) and Piwi, are found associated with this family in addition to N-terminal and middle domains (Song et al., 2004; Song and Joshua-Tor, 2006). The Ago Piwi domain is thought to have an RNase H-type fold (Liu et al., 2004) containing a Mg²⁺ ion to catalyze the cleavage of target RNA (Schwarz et al., 2004).

As there are several Ago proteins contributing to different modes of RNAi, the specific role that many individual Ago proteins fulfill is an active area of investigation (Meister et al., 2004; Tolia and Joshua-Tor, 2007). This is especially relevant for plant–virus interactions (Alvarado and Scholthof, 2009), and thus far, antiviral roles have been suggested for Ago1, Ago7, and Ago4 (Baumberger and Baulcombe, 2005; Baumberger et al., 2007; Bhattacharjee et al., 2009; Bortolamiol et al., 2007; Csorba et al., 2010; Qu et al., 2008). Once RISC is activated, the incorporated siRNA ensures sequence-specific binding to a cognate target ssRNA, followed by Ago-mediated cleavage of the target RNA in a manner similar to that of RNase H, 10-nt in from the 5'-end of the bound siRNA (Ameres et al., 2007).

It is generally hypothesized that during virus infection of eukaryotic hosts, components of the RNAi pathway similar to those outlined above generate virus-derived siRNAs to program an antiviral RISC. Recently, a suppressor-defective mutant of *Tomato bushy stunt virus* (TBSV) (Omarov et al., 2006; Scholthof, 2006; Yamamura and Scholthof, 2005) was used to isolate one such RISC from extracts of infected *Nicotiana benthamiana* plants. Biochemical analysis revealed a discrete RISC-like effector that was associated with TBSV-derived siRNAs and specifically targeted the viral RNA for degradation during *in vitro* reactions (Omarov et al., 2007). This provided direct evidence

* Corresponding author. Fax: +1 979 845 6483.

E-mail address: herscho@tamu.edu (H.B. Scholthof).

¹ Present Address: Graduate Program in Cellular and Molecular Biology, University of Wisconsin, 1525 Linden Drive, Madison, WI 53706, USA.

² Present Address: L. N. Gumilyov Eurasian National University, Munaitpasova 5, Astana 10008, Kazakhstan.

that the anti-TBSV RISC was cleaving the target RNA rather than causing translational repression. Using a somewhat different approach, these findings were independently corroborated for a related tombusvirus (Pantaleo et al., 2007).

It is reasonable to hypothesize that the above processes are not unique to tombusviruses, as specifically illustrated by other virus gene vectors used to trigger virus-induced gene silencing (VIGS) (Batten et al., 2003; Burch-Smith et al., 2004; Ratcliff et al., 2001). Furthermore, many animal and plant viruses encode silencing suppressors (Li and Ding, 2006; Omarov and Scholthof, in press; Scholthof, 2007; Voinnet, 2005), also suggesting they encounter host enforced RNA silencing defenses during infection. Nevertheless, the demonstration of detectable and *in vitro* active antiviral RISC thus far remains unique to the tombusvirus–host system.

To examine the validity of a model predicting the existence of a conserved antiviral silencing pathway in plants and to determine if it corresponds to those based on other systems like *Drosophila*, it is necessary to biochemically analyze the defense response of plants towards different viruses. We hypothesized that an antiviral RISC can be isolated from plants infected with a virus not related to tombusviruses, and analysis of its biochemical characteristics would help to determine if the same or different RISCs target RNAs from different virus species. For this we chose a tobavirus *Tobacco rattle virus* (TRV) variant, which is commonly used as an effective VIGS vector in a wide range of plants (Burch-Smith et al., 2006; Ratcliff et al., 2001).

The results show that column chromatography of extracts from *N. benthamiana* plants infected with TRV yielded fractions exhibiting ribonuclease activity specific for TRV RNA. This activity was inhibited in the presence of NaCl and EDTA, and stimulated by addition of divalent metal cations. Moreover, ribonuclease activity exhibited a preference for longer RNA segments as a cleavage substrate. Interestingly, the specificity of the nuclease activity could be reprogrammed *in vitro* with the addition of total RNA extract from TBSV-infected plants. The evidence strongly supports the view that induction of an antiviral RISC is a common molecular defense pathway and that the composition of this effector is conserved while its specificity is strictly governed by the siRNA content.

Results

Ribonuclease activity associated with siRNAs and Piwi proteins in extracts of TRV-infected plants

To establish TRV infections in *N. benthamiana*, plants were infiltrated with *Agrobacterium* cultures containing T-DNA plasmids that express TRV RNA1 as well as the RNA2 vector with a segment of the *phytoene desaturase* (*pds*) gene (Burch-Smith et al., 2004). Following infiltration of *N. benthamiana*, silencing of *pds* expression is observed as a whitening of tissue (Fig. 1). This type of silencing is virus replication-dependent; agroinfiltrations of the RNA2 construct in absence of RNA1 does not elicit the silencing response (data not shown).

The earliest experiments for this project involved the harvest of tissue at 8 or 2 weeks post-infiltration. Following column chromatography, many fractions exhibited extensive non-specific *in vitro* degradation of any RNA transcripts (data not shown). In an attempt to avoid or minimize non-specific degradation, tissue was harvested from infected *N. benthamiana* plants at the onset of *pds* silencing-induced bleaching, 5 days post-infiltration. Tissue extract was clarified by centrifugation and separated on a 40-ml hydroxyapatite chromatography column. The resultant fractions were individually tested for ribonuclease activity that was still found to be non-specific, as both TRV and TBSV RNAs were degraded (data not shown). These observations suggested that if RISC activity was present, there was insufficient separation from contaminating nucleases, and that additional purification steps were required.

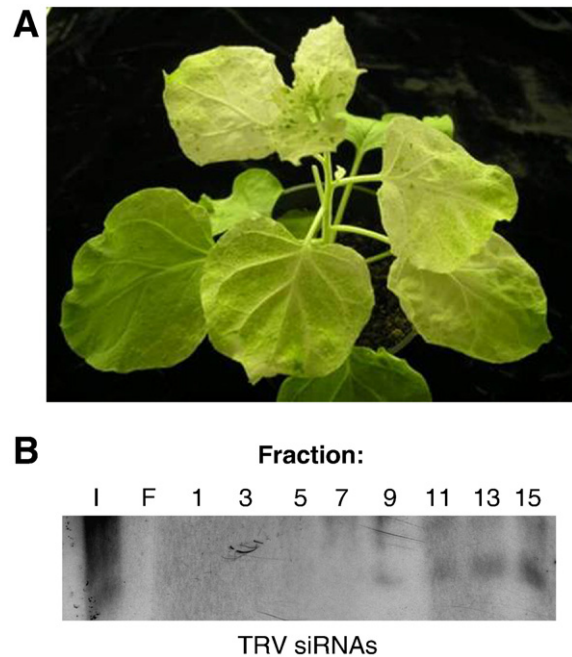


Fig. 1. TRV siRNAs in hydroxyapatite column chromatography fractions from TRV-*pds* infected *N. benthamiana* plants. (A) Image of TRV-*pds* infected plant at 14 days post-infiltration, with the upper leaves displaying bleaching due to *pds* silencing. (B) Infected plant tissue was collected 5 days post-infiltration and RNA was extracted from hydroxyapatite chromatography fractions, separated on a 17% acrylamide SDS-PAGE with 8 M urea, and blotted to a membrane for hybridization with a TRV RNA2 probe. Distinct TRV-derived short RNAs first eluted in fraction 9. I, column input; F, column flow-through.

To determine which fractions to select for further isolation, we tested each for biochemical features characteristic for RISC-associated ribonuclease. First, the presence of short RNAs (including siRNAs) was examined in fractions, followed by Northern hybridization with a TRV RNA2 probe (Fig. 1B). A positive signal for a distinct class of TRV-specific siRNAs was first evident in fraction 9, indicating that an anti-TRV RISC would be present in those fractions, based on our previous observations with TBSV (Omarov et al., 2007). Additionally, because a hallmark of RISC is the presence of one or more Ago proteins containing a conserved Piwi domain, we raised a Piwi-antiserum. When fractions were tested with Western blot assays, fractions 9–13 were enriched for multiple piwi-antiserum reactive proteins (Supplemental Fig. 1).

TRV RNA-specific ribonuclease activity

We realized that neither the ribonuclease test, the siRNA analyses, nor the piwi-Western blot assays by themselves provided sufficient evidence for RISC. However, since hydroxyapatite fractions 9–15 (Fig. 1B) encompassed those positive for all three parameters: i) ribonuclease activity, ii) TRV-derived siRNAs, and iii) piwi-antibody reactive proteins, this strongly suggested the presence of RISC. Therefore, these fractions were combined for further separation. After Sephacryl S-200 HR gel column chromatography, fractions were again tested for ribonuclease activity by incubation with *in vitro* generated TRV or TBSV transcripts. The reactions were then subjected to standard agarose gel electrophoresis followed by Northern blot hybridization with probes for either TRV RNA1 (Fig. 2, top panel) or TBSV (Fig. 2, bottom panel) to examine effects on RNA integrity. The results in Fig. 2 reveal that gel filtration fractions 9–11 exhibit nuclease activity against TRV RNA1 transcripts (also observed for RNA2 transcripts, Fig. 3), while no comparable cleavage of TBSV RNA transcripts was evident. Some residual non-specific activity surfaced only at much lower RNA concentrations and upon prolonged reaction

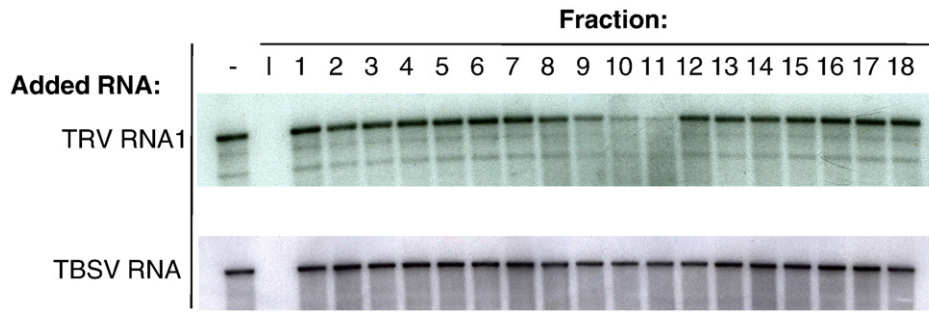


Fig. 2. TRV-specific RISC-nuclease activity. Hydroxyapatite chromatography fractions with nuclease activity and positive for siRNAs and Piwi-like proteins (Fig. S1) were pooled and subjected to Sephacryl S-200 gel filtration. Fractions were then incubated with various types of RNA. Minus (–) indicates transcripts without the addition of any fraction, “I” denotes the addition of the pooled hydroxyapatite sample (column input before Sephacryl S-200 chromatography), and the numbers indicate the fractions to which the RNA was added. Ribonuclease activity was determined by agarose gel electrophoresis of samples followed by Northern blot hybridization with a probe specific for TRV (top) or TBSV (bottom). Added RNA consisted of transcripts representing TRV RNA1 (top) or TBSV genomic RNA (bottom).

incubations. It is noteworthy that these and other supporting gel filtration experiments showed that ribonuclease activity was predominantly associated with fractions representing high MW complexes (200–500 kDa), indicative of a macromolecular composition for RISC. Collectively, the siRNA-associated virus-specific nuclease activity and the macromolecular composition are in agreement with what would be expected for RISC.

To discount the possibility that anti-TRV nuclease activity is a property associated with the use of *in vitro* transcripts or only active against TRV RNA1, experiments were repeated by incubating fraction aliquots with total RNA extracted from TRV-infected *N. benthamiana* plants and RNA2 integrity was determined (Fig. 3, top panel). The results show that fractions 7–10 exhibit nuclease activity towards TRV RNA. These assays were performed with different chromatography preparations than those used in the previous tests (experiments were reiterated with separate sets of infected tissue), and due to column parameters and experimental variations the active fractions elute somewhat earlier from the columns than was presented with Fig. 2.

The results in Fig. 3 provide evidence that the TRV RNA-specific ribonuclease activity associated with the RISC-like preparation is not restricted to the tests with transcripts but also targets viral RNA from plants. In fact, viral RNA from plants appeared to be degraded more efficiently than *in vitro* generated transcripts (Fig. 3). Furthermore, even though both TRV RNA1 (Fig. 2) as well as RNA2 (Fig. 3) transcripts were targets, a reproducible observation was that the ~3 kbp PCR fragment-derived RNA1 transcripts (Fig. 2) were somewhat more efficiently targeted than the ~2 kbp PCR fragment-derived TRV RNA2 transcripts (Fig. 3), especially with prolonged incubations (data not shown).

TRV-RISC activity is inhibited by EDTA and stimulated by divalent metal cations

As the Ago nuclease unit of RISC is thought to be catalyzed by a Mg²⁺ ion, it follows that if this is the case for the anti-TRV RISC,

divalent metal cations would be affected by the addition of the metal chelator EDTA. To test this, EDTA was added in various concentrations to the RISC preparations obtained from hydroxyapatite followed by Sephacryl S-200 chromatographic steps, along with TRV RNA and RNasin-supplemented ddH₂O to measure the effect on the *in vitro* ribonuclease assays (Fig. 4A). The results showed that ribonuclease activity was noticeably reduced by a concentration of 13 mM EDTA, and was fully inhibited in the presence of 20 mM EDTA (Fig. 4A).

We then reasoned that if the nuclease inhibitory effect of EDTA is the sole and specific consequence of chelating divalent cations, then it should be possible to reverse EDTA-mediated inhibition of RISC activity by depleting EDTA with increased concentrations of divalent metal cations. To examine this possibility, assays as above were carried out in presence of increasing concentrations of Mg²⁺ and Mn²⁺ ions, with or without EDTA. The results in Fig. 4B show that Mn²⁺ appears to enhance ribonuclease activity more effectively than Mg²⁺, though both metals stimulated activity at concentrations exceeding 3 mM. The inhibitory effect of EDTA in combination with the stimulatory effect of metals is in agreement with reports that Ago protein-mediated catalysis of RISC requires a divalent metal ion.

Exogenously supplied siRNAs reactivate and reprogram activity-depleted RISC in vitro

The results of Fig. 3 suggested that addition of RNA from TRV-infected plants to RISC fractions resulted in increased aggressive nuclease activity compared to that observed towards *in vitro* generated transcripts. This alluded to a possibility that one or more RISC activity stimulating factors are present in preparations of total RNA from plant extracts that is absent from transcript samples. One obvious factor with the ability to program RISC *in vitro* would be TRV-derived siRNAs introduced into the *in vitro* reaction. Moreover, if this is the case then the reciprocal must occur as well, namely, that depletion of anti-TRV RISC activity *in vitro* should occur after addition

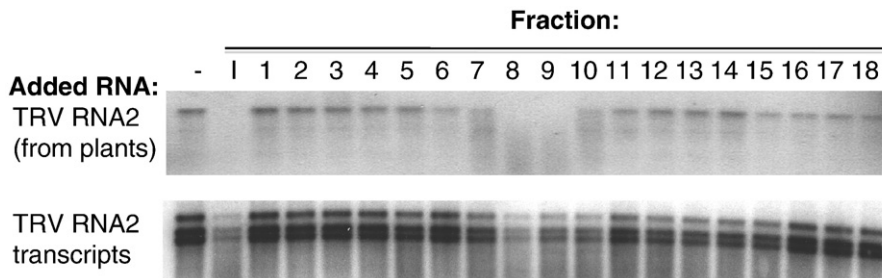


Fig. 3. Susceptibility of TRV RNA isolated from infected plants to *in vitro* RISC-nuclease activity. Active fractions obtained after hydroxyapatite chromatography were pooled and subjected to S-200 chromatography. Subsequently, the obtained fractions (1–18) were incubated with total RNA extracted from TRV-infected *N. benthamiana*, followed by Northern blot assays to measure TRV RNA2 integrity (top), or *in vitro* generated TRV RNA2-*pds* transcripts (bottom). Minus (–) denotes RNA and only ddH₂O; “I” indicates addition of RNA to gel filtration column input (i.e., initially pooled hydroxyapatite samples). For unknown reasons the PCR fragment yielded more than one size transcript.

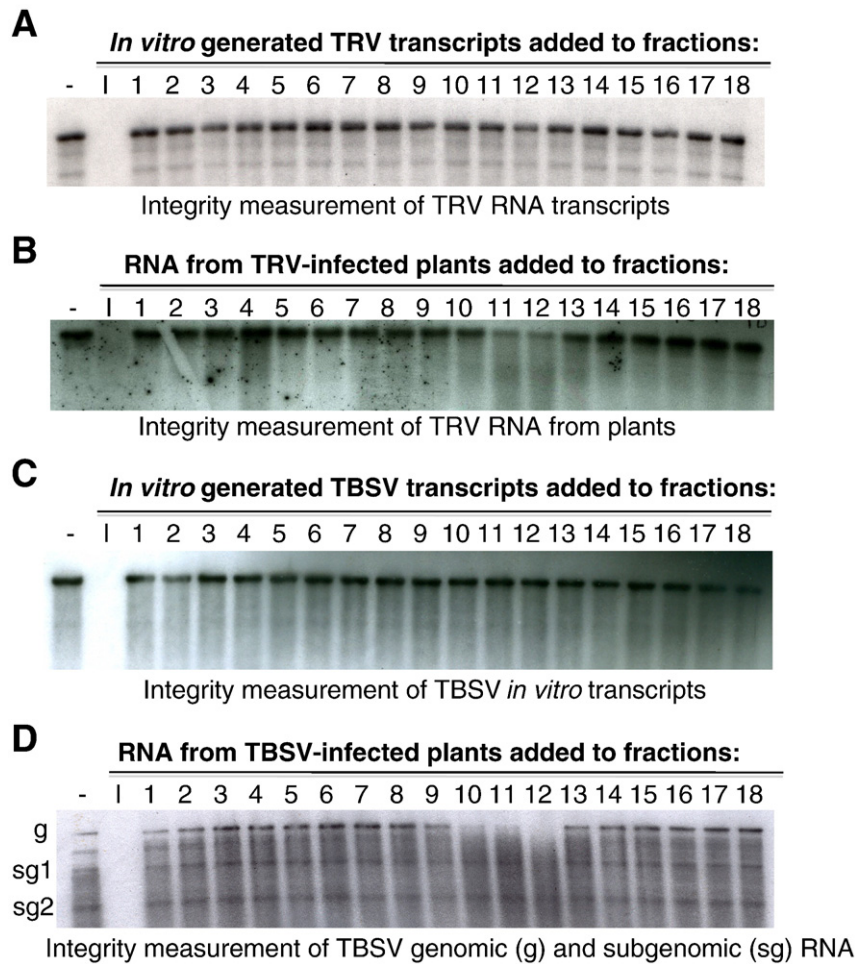


Fig. 5. Inactivation and reprogramming of RISC. (A) Following S-200 chromatography in the presence of 200 mM NaCl, the following RNA substrate was added: (A) TRV RNA1 transcripts, (B) total RNA extracted from TRV-infected *N. benthamiana* plants and assayed for TRV RNA2 by Northern assay, (C) TBSV RNA transcripts, and (D) total RNA extracted from TBSV-infected *N. benthamiana* and assayed by Northern for TBSV RNA. Minus (–) indicates transcripts without the addition of any fraction; “1” denotes the addition of the column input before Sephacryl S-200 chromatography.

previously for TBSV (Omarov et al., 2007), but rough comparisons suggest it to be smaller (<500 kDa). This might reflect a biologically relevant property or it could be due to differences in chromatography treatments that led to dissociation of ancillary proteins from the core anti-TRV RISC nucleosome. Regardless, the TRV RNA degradation in fractions containing the complex is specific, and linked to the presence of siRNAs and Piwi-like proteins. These properties support the interpretation that the fractions contain a functional anti-TRV RISC.

Biochemical properties of the anti-TRV RISC

To provide additional evidence that the anti-TRV complex represents RISC, we tested biochemical properties known to be important for this effector complex. The hypothesis was that if the plant defensive response is RNAi-based, EDTA would act as an inhibitor and Mg^{2+} and Mn^{2+} as stimulants, because the Ago protein of RISC uses metal ions for catalysis of the RNA hydrolysis (Schwarz et al., 2004). The results showed that *in vitro* ribonuclease activity was inhibited with the addition of 20 mM EDTA. Conversely, ribonuclease activity was enhanced by addition of divalent metal cations Mg^{2+} and Mn^{2+} . These properties correspond with the characteristics seen for RISC-like ribonucleases isolated from TBSV-infected plants (Omarov et al., 2007), as well as known properties of RISC proteins (Schwarz et al., 2004).

Even though TRV siRNAs were found in hydroxyapatite chromatography fractions (Fig. 1), detection of these short RNAs proved elusive for the subsequent ribonuclease-active and specific Sephacryl S-200 fractions. This contrasts with our previous observation that siRNAs are readily detectable for the anti-TBSV RISC (Omarov et al., 2007 and data not shown). This difference agrees with the abundant viral siRNA accumulation in TBSV-infected plants (Omarov et al., 2006) compared to the relatively low levels of TRV siRNAs (Fig. 1, and data not shown). A disparity in siRNA generation may also explain difference in silencing suppressor efficiencies reported by others (Donaire et al., 2008). In simple terms, TRV might have a ‘weaker’ silencing suppressor than TBSV and is thus not fully protected (hence its usefulness as a VIGS vector), while the relatively low amount of siRNAs produced corresponds to the less prolific TRV RNA accumulation compared to that observed for TBSV.

The functional assays and biochemical properties suggest that irrespective of the invading virus, TBSV (Omarov et al., 2007) or TRV, *N. benthamiana* plants mount an RNAi response using a RISC with conserved properties. In preliminary attempts to discern if this also holds true for a virus infecting a monocotyledonous host, we infected millet plants with *Panicum mosaic virus* (PMV) (family *Tombusviridae*) and its satellite (SPMV) (Scholthof, 1999). As before, following hydroxyapatite and gel filtration chromatography, fractions were obtained that were enriched for PMV siRNAs and Piwi-reactive proteins (data not shown), and these fractions most specifically targeted PMV RNA for degradation (Supplemental Fig. 2). Collectively, the results

support the notion that antiviral RISCs activated by different viruses in mono- and dicotyledonous plants possess very similar properties.

Reprogramming and size-preference of the antiviral RISC

Biochemical experiments in the present studies showed that fractions from Sephacryl S-200 chromatography, prepared in the presence of 200 mM NaCl to dissociate siRNAs, lost RISC activity. However, the anti-TRV RISC could be reactivated by the addition of total RNA that encompasses siRNAs from TRV-infected plant tissue. If it is true that salt treatment removed siRNAs but left the proteinaceous components of the RISC intact and that the specificity is strictly determined by siRNA content, then an extension of the hypothesis is that siRNA-depleted RISCs should be available for programming with siRNAs unrelated to TRV to gain new sequence specificity. Supportive evidence for this concept was obtained by using the activity-depleted fractions (after treatment with salt to dissociate native siRNAs) and subsequent incubation with total RNA (containing siRNAs) from TBSV-infected plants. This resulted in a strikingly effective recognition and degradation of TBSV RNA, suggesting “re-loading” of the RISC with TBSV siRNAs. These findings support a model that RISC siRNA loading and dissociation can be controlled to adjust the sequence-specific recognition. Our results also clearly favor the interpretation that the association between RISC and siRNAs is not covalent but remains based on electrostatic interactions. The property that RISC can be reprogrammed *in vitro* offers intriguing possibilities to use synthetic siRNAs to custom-design RISC for specific targets *in vitro* and perhaps in the future even *in vivo*, for instance, for various therapeutic purposes.

Even with crude preparations (*sans* salt treatment), there seems to be a population of unprogrammed RISCs present in the same fractions exhibiting activity that can be loaded *in vitro* with the addition of siRNAs to increase activity. This could serve to explain why addition of RNA from TRV-infected plants that also contains TRV siRNAs, causes more aggressive viral RNA degradation than observed for *in vitro* generated transcripts in reactions not supplemented with siRNAs. Along those same lines, the more effective reactivation of RISC activity following addition of RNA from plants infected with TBSV versus that observed upon addition of RNA from TRV-infected plants, agrees with the observation that levels of siRNAs in TRV-infected plants are extremely low (data not shown), while these are abundant in TBSV-infected plants (Omarov et al., 2007).

Irrespective of the notion that siRNAs in the input can be used to “spike” the RISC to become more active or even reprogram the activity, closer inspection of the data warrants the discussion of additional contributing novel properties. For instance, the TRV RNA2-*pds* and transcripts used for the *in vitro* assays are about 2 kb, whereas TRV RNA1 transcripts are ~3 kb; furthermore RNA2 molecules from plants are about 3 kb, whereas RNA1 is even longer. While the shorter RNA transcripts are still targeted by the ribonucleases present in RISC-containing fractions, the longer RNA substrates seem to be targeted more aggressively. Other studies performed with TRV-infected *Arabidopsis* demonstrated that siRNAs are generated along TRV RNA1 heterogeneously, though particularly for the 3'-end (Donaire et al., 2008). This would then favor the targeting of longer viral RNAs from plants with authentic 3'-ends, compared to 3'-truncated shorter transcripts.

Another possibility would be that the preference for longer RNA is an inherent characteristic of the antiviral RISC. For instance, the siRNA distribution along the TBSV genome is fairly uniform (Molnar et al., 2005) with some scattered hot-spots (Szittyta et al., 2010), suggesting no overrepresentation of any region on the genome in the siRNA population. In this context it is unexpected that, just as noted for TRV RNA, the ~5 kb TBSV genomic RNA was the preferred target compared to the shorter sgRNAs (Fig. 5). Therefore, we propose that the preference of the TRV-RISC for longer RNA substrates is not only determined by the siRNA representation but may also be influenced

by a thus far unknown inherent characteristic of the antiviral RISC that remains in place even after the TRV-RISC becomes loaded with siRNAs for a heterologous virus. This feature, as well as the *in planta*-programmed TBSV-activated RISC is the topic of a more detailed study (Omarov et al., to be published) but it is in line with observations for RISC in *Drosophila*, though the transcript sizes cited there ranged only from 100 to 600 nts (Hammond et al., 2000).

Conclusion

As a whole, the findings of this study demonstrate that a virus-specific ribonuclease can be isolated from TRV-infected *N. benthamiana*. This ribonuclease activity is inhibited by EDTA, stimulated in the presence of divalent metal cations, more readily targets longer RNA as a substrate, and can be activated or (re-)programmed by adding RNA isolated from virus-infected plants. Our results support the model that RNA silencing against unrelated viruses in plants deploys a conserved set of processes leading to the programming of a conserved high MW RISC-like effector complex whose specificity is conferred by the siRNA content.

Materials and methods

Infection of plants with TRV and TBSV

Agrobacterium-mediated infection of plants was performed with T-DNA plasmids that express TRV RNA1, and the RNA2 vector with a segment of the *phytoene desaturase* (*pds*) gene (Burch-Smith et al., 2004). Cultures of *Agrobacterium* were grown to an optical density_{600nm} of 2 in Luria broth (LB) and the bacteria were pelleted and re-suspended in 10 ml of 10 mM MES, 10 mM MgCl₂⁺, and 2.25 mM acetosyringone. Equal amounts of TRV RNA1 and TRV RNA2 cultures were combined and three leaves of 3-week-old *N. benthamiana* plants were infiltrated with 1 ml per plant using a needle-less syringe, then grown at 25 °C for 5 days. For TBSV, infectious RNA transcripts were generated (Hearne et al., 1990) using the linearized TBSV DNA as a template [1 μl *Sma*I-linearized DNA was added to 16 μl dd-H₂O, 5 μl 5× transcription buffer, 2.5 μl 5 mM rNTP mix, 2 μl 0.1 mM DTT, 0.25 μl Ribolock RNase inhibitor, and 0.5 μl T7 RNA polymerase (Fermentas, Glen Burnie, MD)]. These transcripts were used to inoculate *N. benthamiana* with RNA-inoculation buffer by lightly rubbing approximately 20 μl on a leaf, as described previously (Hearne et al., 1990; Scholthof et al., 1993).

Column chromatography

For hydroxyapatite chromatography, a column was packed using 40 ml hydroxyapatite bio-gel HT (Bio-Rad, Hercules, CA) in 10 mM sodium phosphate buffer (pH 6.8) in a clean glass column. The column was washed extensively with the same buffer, samples were loaded as outlined below, and fractions were eluted using a 10–200 mM or 10–400 mM (as indicated) increasing sodium phosphate gradient, pH 6.8.

Plants were harvested 5–7 days post-inoculation. About 40 g of tissue from systemically infected plants (including some infiltrated leaves) were ground with a mortar and pestle in 50 ml of 10 mM sodium phosphate buffer, and further processed in a blender with 50 ml additional buffer. This crude extract was filtered through cheesecloth and clarified by centrifugation at 10,000 × g for 20 min at 4 °C. The supernatant was then filtered through cheesecloth into round-bottomed tubes for centrifugation at 14,000 × g for 20 min at 4 °C, when the supernatant was removed and placed on ice until it was loaded on the column. Once all plant extract had been applied to the column (about 100 ml), it was washed thoroughly with 10 mM sodium phosphate buffer, and then proteins were eluted in 3 ml fractions and stored at –20 °C until used.

Proteins in fractions from above were concentrated to 1 ml, using supplier instructions (Amicon Ultrafree-CL, Millipore, Bedford, MA). For Sephacryl S-200 (gel filtration) column chromatography, columns were packed using Sephacryl S200 high resolution resin (Amersham Piscataway, NJ), with 200 mM Tris–HCl, pH 7.4, 5 mM DTT, and the addition of 200 mM of NaCl where indicated. Elution of fractions and their storage used this same buffer.

Extraction of siRNAs from chromatography fractions

For siRNA analysis, 300 μ l of each combined fraction was combined with 1% SDS, incubated at 65 °C for 20 min, then extracted with phenol/chloroform. siRNAs were precipitated with sodium acetate and ethanol and collected using standard centrifugation and washing procedures (Omarov et al., 2006, 2007). The resultant siRNAs were re-suspended in 2:1 formamide/agarose electrophoresis loading dye. Aliquots were loaded on a 17% acrylamide gel containing 8 M urea, and electrophoresis was conducted at 30–45 V in 0.5 \times TBE (45 mM Tris, 45 mM boric acid, 1 mM EDTA) until adequate separation occurred. The RNA was transferred to a nylon membrane using 0.5 \times TBE at 150 mA for 1 h and the membrane was subsequently crosslinked before hybridization.

Total RNA extraction from infected tissue

Total RNA was extracted approximately 1 week post-inoculation for TBSV-infected plants, and 5 days post-infiltration with TRV-*pds* to prevent further degradation of TRV RNA. Approximately 1 g of tissue from systemically infected plants was ground with 1 ml 2 \times STE + 1% SDS (2 mM Tris, 20 mM NaCl, 2 μ M EDTA, and 1% SDS) with chilled mortars and pestles, and RNA was extracted with 1:1 [vol/vol] phenol/chloroform. To precipitate RNA, 8 M lithium chloride was used (Omarov et al., 2007). RNA was re-suspended in dd-H₂O plus 1% RNasin and 2% 0.1 mM DTT (Fermentas, Glen Burnie, MD), to a final concentration of about ~600 ng/ μ l RNA/fraction sample for total RNA additions in activity assays, unless otherwise noted, as determined by Nanodrop (Thermo Fisher Scientific, Wilmington, DE).

RNA transcripts for nuclease activity assays

Ribonuclease activity was assayed using RNA transcripts generated *in vitro* from cDNA. For TRV, PCR reactions were used to amplify segments of TRV RNA1 and RNA2-*pds*, designed to add a 5' T7 polymerase promoter sequence for *in vitro* transcription. The TRV RNA2 forward primer used was 5'-CCGGAATTCCTAATACGACTCACTATAGTCTCTGGTGTG-3', and reverse primer was 5'-CCCGCAATATATATCC-3'. The TRV RNA1 forward primer was 5'-CCGGAATTCCTAATACGACTCACTATAGGCAAGGAAAAACGGTCAACG-3', and the reverse primer was 5'-TTCAATGGAAATAGATTG-3'. The TRV RNA1 forward primers spans positions 2404–2424, with the reverse at 5386–5405, to yield a 3 kbp PCR fragment. For TRV RNA2-*pds*, the forward primer is at nt 811–824 and the reverse primer is at 2494–2509, and the resultant product is about 2 kbp.

DNA was extracted using Qiagen Mini-prep kits (Valencia, CA), and stored at –20 °C until needed. For PCR, primers were diluted to about 50 pM; 1 μ l of the DNA was mixed with 1 μ l of each primer, 1 μ l 12.5 mM dNTP mix, 1 μ l MgSO₄, 5 μ l Thermopol buffer, 40 μ l a/c ddH₂O, and 1 μ l Vent DNA polymerase (2000 U/ml) (New England Biolabs, Ipswich, MA). PCR settings used were 3 min pre-denature at 93 °C, and then cycles of 1 min denature at 93 °C, 1 min re-annealing at 55 °C, and 2 min 15 s extension at 72 °C, for 35 cycles. RNA transcripts were then generated from these PCR templates as described above. TBSV transcripts were generated as outlined for plant inoculation.

Assays for the presence and characterization of ribonuclease activity

Fractions from column chromatography were mixed with either total RNA extracted from virus-infected plants, or with transcripts generated *in vitro* as outlined above. To test for activity of ribonucleases, 5 μ l of each combined fraction was incubated at room temperature (about 25 °C) with 1.5–2 μ l RNA for 20 min in the presence of RNasin-containing dd-H₂O. To test for inhibition by EDTA or NaCl, the indicated amount of 50 mM stock EDTA was added to each fraction before the addition of RNA. To determine the effect of divalent metal cations on ribonuclease activity present in the fractions, 50 mM MgCl₂ or 50 mM MnSO₄ were used in the amount specified by the assay.

Northern blot hybridization with radioactive DNA probes

After visualization with UV, 1% agarose gels were usually blotted to a nylon membrane (Osmotics, Westborough, MA). The membranes were incubated at 65° for regular RNA assays and 41 °C for siRNA blots, and RNA was detected using [³²P]dCTP randomly primed hybridization probes made using the appropriate DNA plasmid. For TRV, the RNA2 encoding segment with only a MCS was used (without *pds* insert). Standard washing procedures (Omarov et al., 2006) were followed by autoradiography.

SDS-PAGE and Western analysis

For SDS-PAGE, protein samples were loaded onto 7.5% polyacrylamide gels, then transferred to a nitrocellulose membrane (Osmotics, Westborough, MA) for Western blot analysis, and transfer was verified by staining of the membrane with Ponceau S (Sigma, St. Louis, MO). The peptide “kivegqrysrlnerq” was used for commercial (Sigma/Genosys, Woodlands, TX) production of Piwi-reactive antibody in rabbits. BLAST analysis of plant Ago proteins showed this peptide to represent a well-conserved plant Ago protein domain. These primary antibodies were added at 1:2000 dilutions for at least 2 h followed by incubation with secondary goat anti-rabbit antibodies conjugated to alkaline phosphatase (Omarov et al., 2006). Blots were developed with 5-bromo-4-chloro-3-indolyl phosphate p-toluidine (BCIP) (66 μ l) and nitroterazolium blue chloride (NTB) (33 μ l) (Sigma-Aldrich, St. Louis, MO) in alkaline phosphate buffer. For chemiluminescence assays, antibody goat-anti-rabbit conjugated to horseradish peroxidase-conjugated was used (Biorad, Hercules, CA) for secondary antibody, and the complex detected by an enhanced chemiluminescence detection kit (Pierce, Rockford, IL).

Supplementary materials related to this article can be found online at doi:10.1016/j.virol.2010.12.018

Acknowledgments

We thank S. Dinesh-Kumar, Peter Moffett, and Rick Nelson for providing TRV constructs, Yi-Cheng (John) Hsieh for providing both discussion and healthy plants, Kristina M. Twigg for laboratory support in various ways, and Veria Alvarado and Karen-Beth G. Scholthof for critical reading of the manuscript, and K-B.G.S. for providing the PMV/SPMV materials. This work was made possible by support from Texas AgriLife Research (TEX08387), and awards from NIH (1R03-AI067384), and USDA/CSREES-NRI-CGP (2006-35319-17211). J.J.C. was a recipient of the Willie May Harris Charitable Trust Graduate Fellowship.

References

- Alvarado, V.Y., Scholthof, H.B., 2009. Plant responses against invasive nucleic acids: RNA silencing and its suppression by plant viral pathogens. *Semin. Cell Dev. Biol.* 20, 1032–1040.

- Ameres, S.L., Martinez, J., Schroeder, R., 2007. Molecular basis for target RNA recognition and cleavage by human RISC. *Cell* 130, 110–112.
- Batten, J.S., Yoshinari, S., Hemenway, C., 2003. Potato virus X; a model system for virus replication, movement, and gene expression. *Mol. Plant Pathol.* 4, 125–131.
- Baulcombe, D., 2004. RNA silencing in plants. *Nature* 431, 356–363.
- Baumberger, N., Baulcombe, D.C., 2005. Arabidopsis ARGONAUTE1 is an RNA slicer that selectively recruits microRNAs and short interfering RNAs. *Proc. Natl Acad. Sci. USA* 102, 11928–11933.
- Baumberger, N., Tsai, C.-H., Lie, M., Havecker, E., Baulcombe, D.C., 2007. The polerovirus silencing suppressor P0 targets Argonaute proteins for degradation. *Curr. Biol.* 17, 1609–1614.
- Bhattacharjee, S., Zamora, A., Azhar, M.T., Sacco, M.A., Lambert, L.H., Moffett, P., 2009. Virus resistance induced by NB-LRR proteins involves Argonaute4-dependent translational control. *Plant J.* 58, 940–951.
- Bortolamiol, D., Pazhouhandeh, M., Marrocco, K., Genschik, P., Ziegler-Graff, V., 2007. The polerovirus F Box protein P0 targets Argonaute1 to suppress RNA silencing. *Curr. Biol.* 17, 1615–1621.
- Burch-Smith, T.M., Anderson, J.C., Martin, G.B., Dinesh-Kumar, S.P., 2004. Applications and advantages of virus-induced gene silencing for gene function studies in plants. *Plant J.* 39, 734–746.
- Burch-Smith, T.M., Schiff, M., Liu, Y., Dinesh-Kumar, S.P., 2006. Efficient virus-induced gene silencing in *Arabidopsis*. *Plant Physiol.* 142, 21–27.
- Csorba, T., Lóza, R., Hutvágner, G., Burgyán, J., 2010. Polerovirus protein P0 prevents the assembly of small RNA containing RISC complexes and leads to the degradation of Argonaute 1. *Plant J.* 62, 463–472.
- Donaire, L., Barajas, D., Martinez-Garcia, B., Martinez-Priego, L., Pagan, I., Llave, C., 2008. Structural and genetic requirements for the biogenesis of Tobacco rattle virus-derived small interfering RNAs. *J. Virol.* 82, 5167–5177.
- Filipowicz, W., 2005. RNAi: the nuts and bolts of the RISC machine. *Cell* 122, 17–20.
- Hammond, S.M., Bernstein, E., Beach, D., Hannon, G.J., 2000. An RNA-directed nuclease mediates post-transcriptional gene silencing in *Drosophila* cells. *Nature* 404, 293–296.
- Hammond, S.M., Boettcher, G., Caudy, A.A., Kobayashi, T., Hannon, G.J., 2001. Argonaute2, a link between genetic and biochemical analyses of RNAi. *Science* 293, 1146–1150.
- Hearne, P.Q., Knorr, D.A., Hillman, B.I., Morris, T.J., 1990. The complete genome structure and synthesis of infectious RNA from clones of tomato bushy stunt virus. *Virology* 177, 141–151.
- Li, F., Ding, S.W., 2006. Virus counterdefense: diverse strategies for evading the RNA-silencing immunity. *Ann. Rev. Microbiol.* 60, 503–531.
- Liu, J., Carmell, M.A., Rivas, F.V., Marsden, C.G., Thomson, J.M., Song, J.-J., Hammond, A.M., Joshua-Tor, L., Hannon, G.J., 2004. Argonaute 2 is the catalytic engine of mammalian RNAi. *Science* 305, 1437–1441.
- MacRae, I., Ma, E., Zhou, M., Robinson, C.V., Doudna, J.A., 2008. *In vitro* reconstitution of the human RISC-loading complex. *Proc. Nat. Acad. Sci. U.S.A.* 105, 512–517.
- Meister, G., Landthaler, M., Patkaniowska, A., Dorsett, Y., Teng, G., Tuschl, T., 2004. Human Argonaute2 mediates RNA cleavage targeted by miRNAs and siRNAs. *Mol. Cell* 23, 1437–1441.
- Molnar, A., Csorba, T., Lakatos, L., Varallyay, E., Lacomme, C., Burgyan, J., 2005. Plant virus-derived small interfering RNAs originate predominantly from highly structured single-stranded viral RNAs. *J. Virol.* 79, 7812–7818.
- Omarov, R.T., and Scholthof, H.B., in press. Biological chemistry of virus-encoded RNA silencing suppressors: an overview. *Meth. Mol. Biol.*
- Omarov, R., Sparks, K., Smith, L., Zindovic, J., Scholthof, H.B., 2006. Biological relevance of a stable biochemical interaction between the tobusvirus-encoded P19 and short interfering RNAs. *J. Virol.* 80, 3000–3008.
- Omarov, R.T., Ciomperlik, J.J., Scholthof, H.B., 2007. RNAi-associated ssRNA-specific ribonucleases in *Tombusvirus* P19 mutant-infected plants and evidence for a discrete siRNA-containing effector complex. *Proc. Natl Acad. Sci. USA* 104, 1714–1719.
- Pantaleo, V., Szittyta, G., Burgyan, J., 2007. Molecular bases of viral RNA targeting by viral small interfering RNA-programmed RISC. *J. Virol.* 81, 3797–3806.
- Qu, F., Ye, X., Morris, T.J., 2008. Arabidopsis DRB4, AGO1, AGO7, and RDR6 participate in a DCL4-initiated antiviral RNA silencing pathway negatively regulated by DCL1. *Proc. Natl Acad. Sci. USA* 105 (38), 14732–14737.
- Ratcliff, F., Martin-Hernandez, A.M., Baulcombe, D., 2001. Tobacco rattle virus as a vector for analysis of gene function by silencing. *Plant J.* 25, 237–245.
- Romano, N., Macino, G., 1992. Quelling: transient inactivation of gene expression in *Neurospora crassa* by transformation with homologous sequences. *Mol. Microb.* 6, 3343–3353.
- Scholthof, K.-B.G., 1999. A synergism induced by satellite panicum mosaic virus. *Mol. Plant-Microbe Interact.* 12, 163–166.
- Scholthof, H.B., 2006. The *Tombusvirus*-encoded P19: from irrelevance to elegance. *Nat. Rev. Microbiol.* 4, 405–411.
- Scholthof, H.B., 2007. Heterologous expression of viral RNA interference suppressors; RISC management. *Plant Physiol.* 145, 1110–1117.
- Scholthof, H.B., Morris, T.J., Jackson, A.O., 1993. The capsid protein gene of tomato bushy stunt virus is dispensable for systemic movement and can be replaced for localized expression of foreign genes. *Mol. Plant-Microbe Interact.* 6, 309–322.
- Schwarz, D.S., Tomari, Y., Zamore, P.D., 2004. The RNA-induced silencing complex is a Mg²⁺-dependent endonuclease. *Curr. Biol.* 14, 787–791.
- Song, J.J., Joshua-Tor, L., 2006. Ago and RNA—getting into the groove. *Curr. Opin. Biol. Rev.* 16, 5–11.
- Song, J.-J., Smith, S.K., Hannon, G.J., Joshua-Tor, L., 2004. Crystal structure of Argonaute and its implications for RISC slicer activity. *Science* 305, 1434–1437.
- Szittyta, G., Moxon, S., Pantaleo, V., Toth, G., Rusholme-Pilcher, R.L., Moulton, V., Burgyan, J., Dalmay, T., 2010. Structural and functional analysis of viral siRNAs. *PLoS Pathog.* 6, 1–15.
- Tolia, N.H., Joshua-Tor, L., 2007. Slicer and the Argonauts. *Nat. Chem. Biol.* 3, 36–43.
- Tomari, Y., Du, T., Zamore, P.D., 2007. Sorting of *Drosophila* small silencing RNAs. *Cell* 130, 299–308.
- Voinnet, O., 2005. Induction and suppression of RNA silencing: insights from viral infections. *Nat. Rev. Genet.* 6, 206–220.
- Yamamura, Y., Scholthof, H.B., 2005. Pathogen profile: tomato bushy stunt virus: a resilient model system for studying virus–plant interactions. *Mol. Plant Pathol.* 6, 491–502.